

Peter L. Gonthier · Sarah A. Story · Brian D. Clow · Alice K. Harding

# Population statistics study of radio and gamma-ray pulsars in the Galactic plane

Received: date / Accepted: date

**Abstract** We present results of our pulsar population synthesis of ordinary isolated and millisecond pulsars in the Galactic plane. Over the past several years, a program has been developed to simulate pulsar birth, evolution and emission using Monte Carlo techniques. We have added to the program the capability to simulate millisecond pulsars, which are old, recycled pulsars with extremely short periods. We model the spatial distribution of the simulated pulsars by assuming that they start with a random kick velocity and then evolve through the Galactic potential. We use a polar cap/slot gap model for  $\gamma$ -ray emission from both millisecond and ordinary pulsars. From our studies of radio pulsars that have clearly identifiable core and cone components, in which we fit the polarization sweep as well as the pulse profiles in order to constrain the viewing geometry, we develop a model describing the ratio of radio core-to-cone peak fluxes. In this model, short period pulsars are more cone-dominated than in our previous studies. We present the preliminary results of our recent study and the implications for observing these pulsars with GLAST and AGILE.

**Keywords** pulsars ·  $\gamma$ -rays sources · pulsar populations · nonthermal radiation mechanisms

**PACS** 97.60.Gb · 97.60.Jd · 95.30.Gv

P.L. Gonthier · S.A. Story · B.D. Clow  
Hope College, Department of Physics, 27 Graves Place, Holland, MI 49424  
Tel.: 616-395-7142  
Fax: 616-395-7123  
E-mail: gonthier@hope.edu, sarah.story@hope.edu, brian.clow@hope.edu

A. Harding  
NASA Goddard Space Flight Center, Laboratory for High Energy Astrophysics, Greenbelt, MD 20771  
Tel.: 301-286-7824  
Fax: 301-286-1682  
E-mail: harding@twinkie.gsfc.nasa.gov

---

## 1 Introduction

In the very near future, the  $\gamma$ -ray telescopes AGILE and GLAST will be launched. It is expected that the number of identified  $\gamma$ -ray pulsars will greatly increase. The  $\gamma$ -ray pulsar Geminga appears to be radio silent or at least very weak. It is not clear whether its radio quiet nature is caused by a misalignment of  $\gamma$ -ray and radio beams due to viewing geometry, or by intrinsically weak radio emission. In the past, polar cap models [5] located the  $\gamma$ -ray emission along the same open field lines as radio emission at similar altitudes. In such a model, the  $\gamma$ -ray and radio beams are coaxial with a large overlap, predicting a larger number of radio-loud than radio-quiet  $\gamma$ -ray pulsars. On the other hand, the  $\gamma$ -ray emission region in the outer gap models [20][3] is located near the light cylinder where the  $\gamma$ -ray beam is at a large angle relative to the radio beam that leads the viewer to observe high-energy and radio emission originating from opposite poles. The outer gap model predicts a much larger number of radio-quiet than radio-loud  $\gamma$ -ray pulsars. Thus the ratio of radio-loud to radio-quiet  $\gamma$ -ray pulsars could serve as a discriminating signature to distinguish between competing models.

---

## 2 Simulation - Assumptions

The present simulations are extensions of previous works by Gonthier et al. ([7], [8] & [10]) that include both normal, isolated and millisecond pulsars from the Galactic disk, and the emission of  $\gamma$ -rays within the slot gap/polar cap model. Two years ago at the Hong Kong meeting [9], we presented simulations of pulsars from the Gould Belt accounting for less than 30% of the EGRET unidentified  $\gamma$ -ray sources that were previously correlated to the location of the Gould Belt. Recent reassessment of the diffuse  $\gamma$ -ray background by Casandjian & Grenier [2] suggests that the Gould Belt is no longer such a significant source of EGRET unidentified  $\gamma$ -ray sources. As a result, we do not simulate pulsars from the Gould Belt in this study.

For both normal and millisecond (ms) pulsars, we assume a birth location in the Galactic disk as given by Paczyński [19]. We evolve the neutron stars from their birth location to the present in the Galactic potential defined by Dehnen & Binney [6]. For normal pulsars, we assume a supernova kick velocity distribution of Hobbs et al. [13], a uniform initial period distribution from 0 to 500 ms, initial magnetic field distributions with a decay constant as given in Gonthier et al. [8] and a uniform birth rate back to 1 Gyr.

For ms pulsars, we begin the evolution by using the magnetic field and supernova kick velocity distributions of Cordes & Chernoff [4]. Recent studies of low-mass X-ray binary systems (LMXBs) have been able to determine the spins of the accreting neutron stars allowing for an estimate of their magnetic fields. Lamb & Yu [17] conclude that the properties of these LMXBs are consistent, if they have magnetic fields between  $3 \times 10^7$  G and  $3 \times 10^8$  G and accretion rates ranging from the Eddington critical rate  $\dot{M}_E$  to  $3 \times 10^{-3} \dot{M}_E$ . These different accretion rates result in different birth lines in the  $P - \dot{P}$  diagram (see figure 4 in Lamb & Yu [17]). We have included an approximate procedure to take into account this distribution of accretion rates by dithering the intercept of the birth line described as

$$\log(\dot{P}) = \frac{4}{3} \log(P) - 14.9. \quad (1)$$

While we tried a Gaussian distribution of the birth line, we obtained better agreement with a uniform distribution of birth lines between  $\dot{M}_E$  to  $3 \times 10^{-3} \dot{M}_E$  [17]. We assume a uniform birth rate for ms pulsars back to 12 Gyr. We explore various power laws of the magnetic field distribution getting better agreement with  $n(B) \propto B^{-1}$  and with a  $B_{min} = 2 \times 10^8$  G. Given the magnetic field, a selected birth line and the pulsar age, we obtain the present period and period derivative.

We use a larger Galactic scale height of 200 pc for ms pulsars, compared to the one used for normal pulsars of 75 pc [19]. Since the supernova kick velocities of ms pulsars are much smaller than those of normal pulsars, most ms pulsars remain bound to the Galaxy, oscillating in and out of the Galactic plane with time. We evolve a large number of neutron stars generated in our Monte Carlo simulation to determine the equilibrium spatial distribution of ms pulsars, which we then use in subsequent simulations. A scale height of 410 pc of the evolved ms pulsars is in good agreement with a scale height of 500 pc (exponential scale) of Cordes & Chernoff [4] and with a scale height of 410 pc of LMXBs [11].

For the radio luminosity, we assume that radio pulsars are standard candles and follow the prescription of Arzoumanian, Chernoff & Cordes [1] (ACC) given by the expression

$$L = 2.1 \times 10^{12} P^{-1.3} \dot{P}^{0.4} \text{mJy} \cdot \text{kpc}^2 \cdot \text{MHz}. \quad (2)$$

However, to obtain good agreement between the measured and simulated flux and distance distributions, we

needed to reduce the luminosity by a factor of 73 and 200 for normal pulsars and ms pulsars, respectively. We follow the geometric model of the core beam in ACC [1] and the cone model of Kijak & Gil [16] described in this meeting by Harding, Grenier, & Gonthier [12]. In the study of ACC, the ratio of the core-to-cone peak fluxes had a  $P^{-1}$  dependence, resulting in a dominance of the core component for short period pulsars. As discussed by Harding et al. [12], we find compelling evidence that short period pulsars are more cone dominated than in the ACC model and have adopted a different model to characterize this relationship (see [12]).

The “detection” of our simulated radio pulsars is accomplished using the characteristics of ten radio surveys, six of which are at a frequency around 400 MHz - Arecibo 3, Arecibo 2, Greenbank 2, Greenbank 3, Molongo 2 and Parkes 2, and four surveys are around 1400 MHz - Parkes 1, Jodrell Bank 2, Parkes Multibeam, and we have recently added the Swinburne Intermediate Latitude survey at 1400 MHz. These surveys provide us with 1208 normal and 50 ms pulsars to which we normalize our simulation. We adjust the radio luminosity using only the Parkes MB pulsar survey in order to get a neutron star birth rate of about 2 per century. This survey has over 800 detected pulsars, and we have the best description of the minimum radio flux  $S_{min}$  of the ten surveys. Normalization to 1208 radio pulsars seen by the group of 10 surveys is then the only overall adjustment made, thereby, allowing the prediction of birth rates, radio-loud and radio-quiet  $\gamma$ -ray pulsars detected by the instruments EGRET, AGILE and GLAST. Simulated neutron stars whose radio flux is below the survey threshold,  $S_{min}$ , are assumed to be radio-quiet.

The simulation of the  $\gamma$ -ray emission occurs over two regions in the  $P - \dot{P}$  diagram separated by the curvature radiation pair death line (CRPDL), below which the curvature radiation  $\gamma$  rays no longer produce electron-positron pairs. Above this death line, emission originates from low altitude pair cascades on the inner edge of the slot gap [8], as well as from primaries accelerating in the slot gap at high altitude forming a caustic component [12]. Below this death line, the slot gap dissolves due to the less effective screening of the electric field, leading to extended emission over the entire polar cap. The  $\gamma$ -ray emission above CRPDL is most important for normal pulsars while emission below the CRPDL is the dominant  $\gamma$ -ray emission mechanism for ms pulsars.

The simulated  $\gamma$ -ray flux is compared to the all sky threshold maps for EGRET, AGILE and GLAST. We include the revised EGRET map that includes the dark clouds (see [2]) and the revised GLAST map (after DC2) without the dark clouds (Grenier private communication). The all sky map for AGILE (Pellizzoni private communication) has not been recently updated.

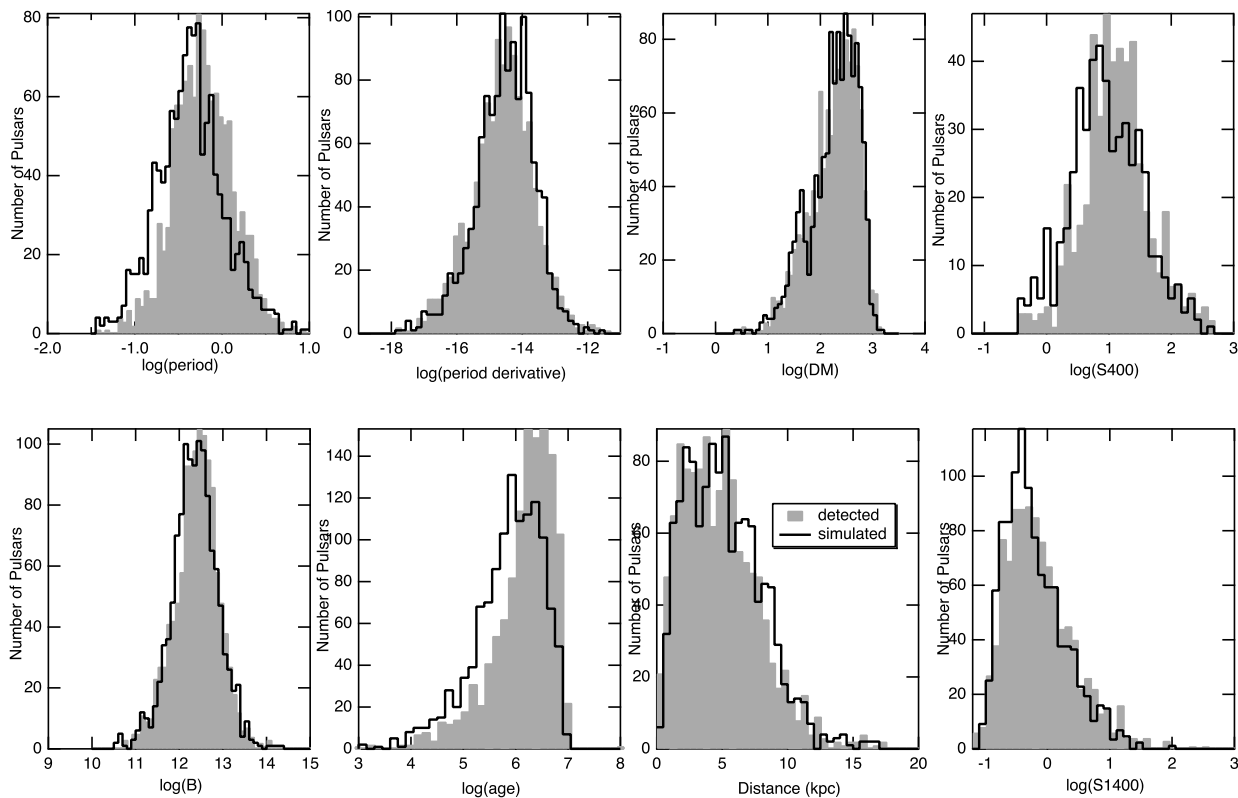


**Fig. 1** Distributions of various characteristics of normal pulsars indicated as detected pulsars (shaded histograms) and simulated (unshaded histograms) pulsars from the Galactic plane.

### 3 Results

In Figure 1, we compare simulated distributions (unshaded histograms) of various characteristics of normal pulsars with those detected (shaded histograms) by the select group of 10 radio surveys. For the flux distributions at 400 and 1400 MHz, we have used the values given in the ATNF pulsar catalog for the detected distributions. In the simulation, we assign a flux at 400 MHz if the pulsar is detected by one of the low frequency surveys in our group and likewise for the fluxes at 1400 MHz. As can be seen in the comparisons of these distributions, the model simulation over-predicts the number of young pulsars with short periods. The distance distribution is now much improved from our previous results [10] mainly due to the inclusion of the actual width of the simulated pulse profile of each pulsar in the calculation of the survey flux threshold,  $S_{\min}$ . Overall we generally see good agreement between the simulation and detected distributions with a predicted birth rate of 1.8 normal pulsars per century.

The simulation again overestimates the number of young and distant ms pulsars as shown in Figure 2. Evident in the histograms is the limitation of a sample of 50 ms pulsars detected by the select group of ten radio sur-

veys. We simulate 500 ms pulsars and then normalize to the detected 50 in order to obtain smoother histograms for the simulated pulsars. The simulation again overestimates young ms pulsars that are more distance than those detected. The 400 MHz surveys in the simulation seem to be a bit too sensitive. The predicted birth rate is  $6.8 \times 10^{-4}$  per century, which is very close to the birth rates estimated by Lorimer [18] of  $2.9 \times 10^{-4}$  per century and by Kiel & Hurley [15] of  $6.5 \times 10^{-4}$  per century of neutron stars from LMXBs.

In Figure 3, we present the Aitoff plots and  $P - \dot{P}$  diagrams for detected (left) and simulated (right) normal (dots) and MS (crosses) pulsars. Both simulated normal and ms pulsar distributions in the Galaxy are similar to the distributions of those detected. As ms pulsars are closer than normal pulsars, they appear with a larger out-of-plane distribution. We are not quite able to reproduce the “bunching” of ms pulsars with periods between 2 and 10 ms. However, the uniform distribution of the birth line as suggested by Lamb & Yu [17] does seem to be important in order to get fairly good agreement in the  $P - \dot{P}$  diagram with detected ms pulsars. The distribution of detected normal pulsars in the  $P - \dot{P}$  diagram is more or less reproduced by the simulation, but the simulated distribution is too broad in period with too few high-field pulsars. We do find that magnetic field decay

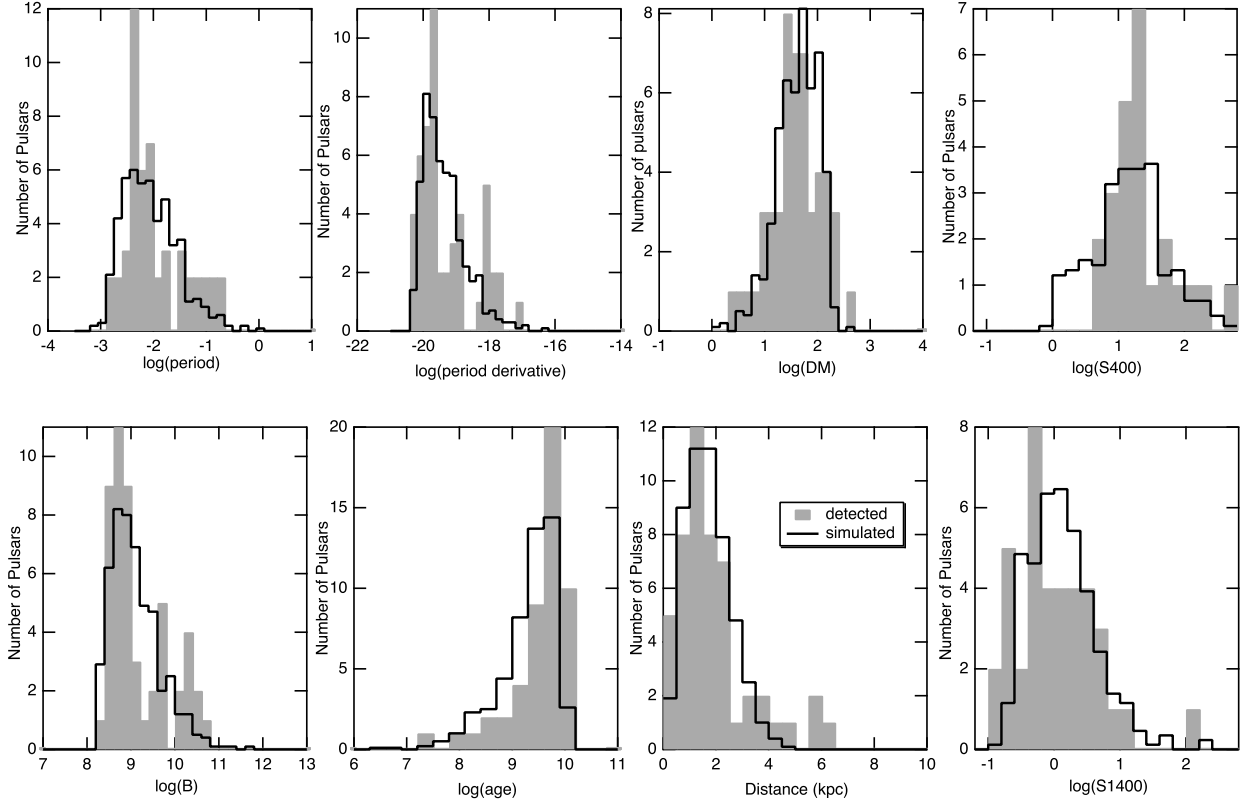


**Fig. 2** Distributions of various characteristics of millisecond pulsars indicated as detected (shaded histograms) and simulated (open histograms) pulsars from the Galactic plane.

with a decay constant of 2.8 Myr is necessary for normal pulsars in order to reproduce the detected distribution. We did not incorporate field decay in the simulation of ms pulsars.

In Table 1, we present the simulated normal and ms  $\gamma$ -ray pulsar statistics for radio-loud and radio-quiet  $\gamma$ -ray pulsars for various instruments indicated as well as the ones detected by EGRET. For normal pulsars, we show separately the number of  $\gamma$ -ray pulsars having detected emission from the low altitude and high altitude slot gap, as both of these radiation mechanisms contribute above the curvature radiation pair death line. As expected the low altitude slot gap beam is more co-axial with the radio beam geometry and results in a greater number of radio-loud  $\gamma$ -ray pulsars. On the other hand, the high altitude emission of the slot gap occurs along the last open field lines all the way out to the light cylinder, at which point the  $\gamma$ -ray beam makes a larger angle to the radio beam and more radio-quiet  $\gamma$ -ray pulsars are detected. In this respect, the high altitude emission of the slot gap resembles the correlations of radio and  $\gamma$ -ray beams of outer gap emission.

The ms  $\gamma$ -ray pulsars in the  $P - \dot{P}$  diagram appear below the curvature radiation pair death line and, therefore, their  $\gamma$ -ray emission arises from the emission over

the entire polar cap region as the slot gap geometry disappears near the curvature death line.

## 4 Conclusions

We present the preliminary results of a population synthesis study of both normal and millisecond pulsars. We include a radio beam geometry that includes a single core and a single cone beam with a new dependence on the core-to-cone peak fluxes. In this new model, as discussed in this conference by Harding et al. [12], short period pulsars are more cone dominated than in our previous studies that follow the ACC model [1]. This relationship is especially important for millisecond pulsars. We use the same radio model for both normal and millisecond pulsars. We describe the radio luminosity using the prescription of ACC (Equation 2), but with luminosity decreased by a factor of 73 and 200 for normal and ms pulsars, respectively, to achieve reasonable neutron star birth rates, flux and distance distributions. The same set of parameters are then used in the simulation of normal and millisecond pulsars. The simulations are run until the same number of normal or millisecond radio pulsars are simulated as detected by a select group of ten radio

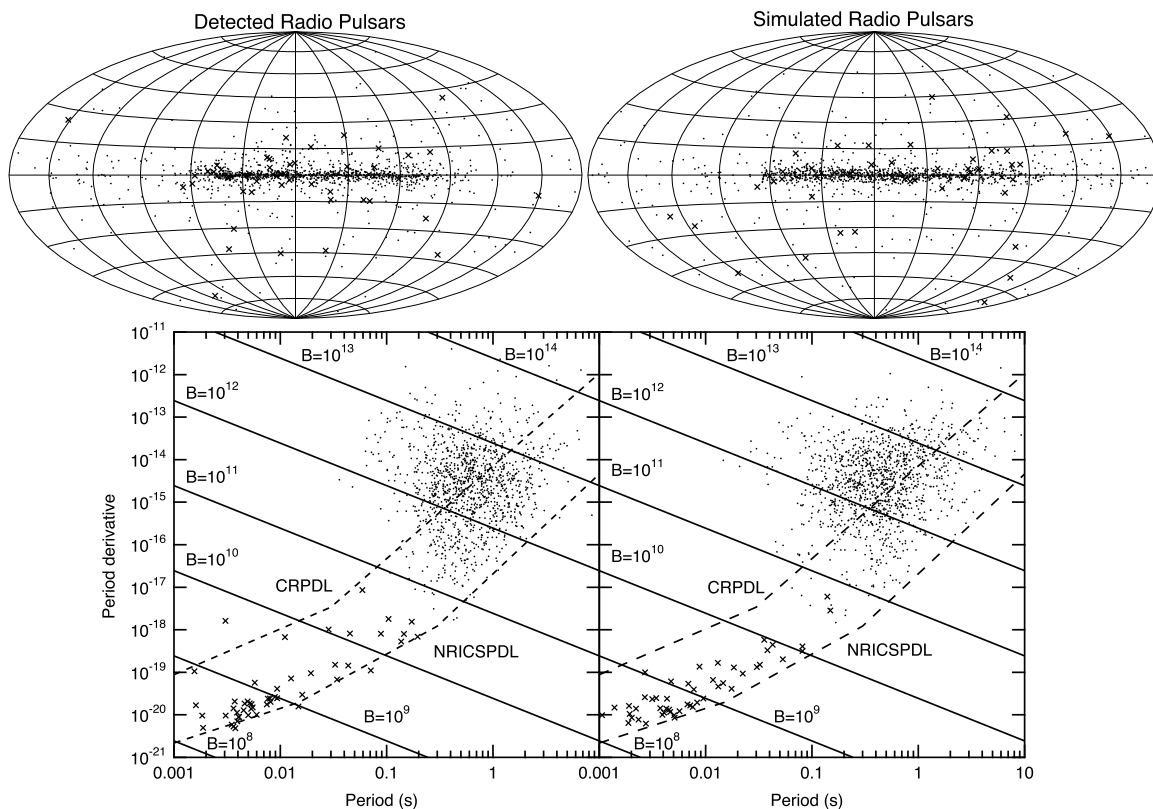


**Fig. 3** Aitoff plots of normal (dots) and millisecond (crosses) pulsars detected (left) by the select group of ten radio surveys and simulated (right). Lower plots are the  $P - \dot{P}$  diagrams of normal (dots) and millisecond (crosses) pulsars detected (left) and simulated (right). Dashed lines represent the pair death lines for curvature radiation (CRPDL) and for nonresonant inverse Compton scattering (NRICSPDL). Solid lines represent the traditional magnetic surface field strength, assuming a constant dipole spin-down field.

**Table 1** Simulated radio-loud and radio-quiet  $\gamma$ -ray pulsar statistics

	Normal Pulsars low + high altitude		Millisecond Pulsars	
Instrument	Radio-Loud	Radio-Quiet	Radio-Loud	Radio-Quiet
EGRET Detected	6	1	1	0
EGRET Simulated	25+2	10+22	1	2
AGILE Simulated	51+1	16+53	2	3
GLAST Simulated	94+6	51+100	4	10

surveys providing an overall normalization of the simulation. With the same set of parameters for the radio beam geometry and luminosity, we achieve very reasonable agreement with the detected distributions of various pulsar characteristics for both normal and millisecond pulsars. This conclusion is quite remarkable.

However, we expect the radio beam geometry of millisecond pulsars to be significantly different, especially for pulsars with periods less than 100 ms, due to the special relativistic effects of aberration, time delays and the sweepback of the magnetic field. These effects and their

contributions are discussed in this meeting by Harding et al. [12]. We hope to soon include this component to the radio emission in our Monte Carlo code to more adequately describe millisecond pulsars.

In previous studies, we only included low altitude  $\gamma$ -ray emission from the slot gap/polar cap model. Both curvature and synchrotron radiation contribute along the last open field line about three stellar radii above the surface resulting in a conical beam symmetric about the magnetic axis. As a result, the  $\gamma$ -ray beam is strongly correlated to the core and cone radio beams assumed

in our simulations. Such a correlation is reflected in the larger number of radio-loud than radio-quiet  $\gamma$ -ray pulsars with a ratio of radio-loud to radio-quiet of 1.8. As discussed by Harding et al. [12] at this meeting, the electric field parallel to the magnetic field along the very last open field lines is not screened, forming a especially narrow slot gap in the case of short period pulsars. The  $\gamma$ -ray beams at high altitude are concentrated (caustic) along the last open field lines with the beam being at large angle to the radio emission. High altitude  $\gamma$ -ray emission then leads to a larger number of radio-quiet  $\gamma$ -ray pulsars being simulated by this mechanism with a ratio of radio-loud to radio-quiet of about 0.06 for this component as indicated in Table 1. The viewing geometry defining the impact angle will determine the respective contributions of the low and high altitude emission. These components will have different signatures in their pulse profiles.

EGRET saw pulsed emission from only one  $\gamma$ -ray ms pulsar, J0218+4342. Though not very optimistic, the simulations predict that GLAST should detect of the order of 10 ms pulsars as point sources. Of the 10 radio-quiet  $\gamma$ -ray ms pulsars only 1 is expected to be detected through blind searches.

Our study of normal, isolated pulsars indicates that GLAST will be able to detect about 100 radio-loud and 151 radio-quiet  $\gamma$ -ray pulsars. These numbers are significantly lower than presented in Gonthier et al.[8], primarily because the new GLAST point-source detection threshold is higher after the great detailed study of the GLAST second data challenge (DC2). The challenge for GLAST will be to detect the radio-quiet  $\gamma$ -ray pulsars through its ability to perform blind searches with those pulsars whose  $\gamma$ -ray fluxes are higher than  $10^{-7}$  photons/(cm<sup>2</sup>·s) (Grenier private communication). Out of the 151 radio-quiet  $\gamma$ -ray pulsars GLAST should be able to detect pulsations in 50 pulsars. The simulation modeling the high and low altitude  $\gamma$ -ray emission within the theoretical framework of the polar cap model suggests that the expected ratio of radio-loud to radio-quiet  $\gamma$ -ray pulsars is about 1.5, while the outer gap models predict many more radio-quiet  $\gamma$ -ray pulsars and a ratio of about 0.1 radio-loud to radio-quiet  $\gamma$ -ray pulsars is expected [14]. Note that the outer gap ratio is similar to the ratio for the high altitude emission alone. Further detailed studies of the correlations between the light curves of radio and  $\gamma$ -ray pulses may provide the best signature to distinguish between the outer gap and polar cap models.

**Acknowledgements** We express our gratitude for the generous support of the Michigan Space Grant Consortium, of Research Corporation (CC5813), of the National Science Foundation (REU and AST-0307365) and the NASA Astrophysics Theory Program.

## References

1. Arzoumanian, Z., Chernoff, D.F. & Cordes, J.M.: The velocity distribution of isolated radio pulsars. *ApJ* **568** 289–301 (2002)
2. Casandjian, J. & Grenier, I.A.: The pulsar contribution to the new EGRET gamma-ray sources. *ApSS*, this meeting, accepted
3. Cheng, K.S., Ruderman, M., & Zhang, L.: A three-dimensional outer magnetospheric gap model for gamma-ray pulsars: geometry, pair production, emission morphologies, and phase-resolved spectra. *ApJ* **537**, 964–976 (2000)
4. Cordes, J.M. & Chernoff, D.F.: Neutron star population dynamics. I millisecond pulsars. *ApJ* **482**, 971–992 (1997)
5. Daugherty, J.K. & Harding, A.K.: Gamma-Ray Pulsars: Emission from Extended Polar CAP Cascades. *ApJ* **458**, 278–292 (1996)
6. Dehnen, W. & Binney, J.: Mass models of the Milky Way. *MNRAS* **294**, 429–438 (1998)
7. Gonthier, P.L., Ouellette, M.S., Berrier, J., O’Brien, S. & Harding, A.K.: Galactic populations of radio and gamma-ray pulsars in the polar cap model. *ApJ* **565**, 482–499 (2002)
8. Gonthier, P.L., Van Guilder, R. & Harding, A.K.: Role of beam geometry in population statistics and pulse profiles of radio and gamma-ray pulsars. *ApJ* **604**, 775–790 (2004)
9. Gonthier, P.L., Van Guilder, R., Harding, A.K., Grenier, I.A. & Perrot, P.A.: Radio-loud and radio-quiet gamma-ray pulsars from the Galaxy and the Gould Belt. *ApSS* **297**, 71–80 (2005)
10. Gonthier, P.L., Story, S.A., Giacherio, B.M., Arevalo, R.A. & Harding, A.K.: Developing radio beam geometry and luminosity models of pulsars. *Chin. J. Astron. Astrophys.* in press
11. Grimm, H.-J., Gilganov, M., & Sunyaev, R.: The Milky Way in X-rays for an outside observer Log(N)-Log(S) and luminosity function of X-ray binaries from RXTE?ASM data. *A&A* **391**, 923–944 (2002)
12. Harding, A.K., Grenier, I.A., & Gonthier, P.L.: The Geminga fraction. *ApSS*, this meeting, accepted
13. Hobbs, G., Lorimer, D.R., Lyne, A.G., & Kramer, M.: A statistical study of 233 pulsar proper motions. *MNRAS* **360**, 974–992 (2005)
14. Jiang, Z.J., & Zhang, L.: Statistical properties of high-energy radiation from young pulsars. *ApJ* **643**, 1130–1138 (2006)
15. Kiel, P.D. & Hurley, J.R.: Populating the Galaxy with low-mass X-ray binaries. *MNRAS* **369**, 1152–1166 (2006)
16. Kijak, J. & Gil, J.: Radio emission regions in pulsars. *MNRAS* **299**, 855–861 (1998)
17. Lamb, F.K. & Yu, W.: Spin Rates and Magnetic Fields of Millisecond Pulsars. In: Rasio, F.A. and Stairs, I.H. (eds.) *Proceedings of Binary Radio Pulsars ASP Conference Series*, Aspen, Colorado, 11-17 January 2004, 299–310. *Astronomical Society of the Pacific*, San Francisco (2005)
18. Lorimer, D.R.: Binary and Millisecond Pulsars. *Living Rev. Relativity* **8**, 7 (2005) <http://www.livingreviews.org/lrr-2005-7>
19. Paczyński, B.: A test of the Galactic origin of gamma-ray bursts. *ApJ* **348**, 485–494 (1990)
20. Romani, R.W., & Ydigaroglu, I.-A.: Gamma-ray pulsars: emission zones and viewing geometries. *ApJ* **438**, 314–321 (1995)